

# Probing black hole X-ray binaries with the Keck telescopes

Emilios T. Harlaftis<sup>a</sup> and Alexei V. Filippenko<sup>b</sup>

<sup>a</sup>Institute of Astronomy and Astrophysics, National Observatory  
of Athens, P. O. Box 20048, Athens - 118 20, Greece

<sup>b</sup>Department of Astronomy, University of California, Berkeley, CA 94720-3411, USA

## ABSTRACT

The advent of the large effective apertures of the Keck telescopes has resulted in the determination with unprecedented accuracy of the mass functions and mass ratios of faint ( $R \approx 21$  mag) X-ray transients (GS 2000+25, GRO J0422+32, Nova Oph 1977, Nova Vel 1993), as well as constraining the main-sequence companion star parameters and producing images of the accretion disks around the black holes.

**Keywords:** black hole physics, interacting binaries, novae, X-ray binaries, X-ray transients, Nova Oph 1977, GS 2000+25, GRO J0422+32, Nova Vel 1993

## 1. INTRODUCTION

Zel'dovich and Novikov (1966) were the first to propose the technique which is still in use for “weighing” black holes. They suggested that black holes could be detected indirectly from light emitted through the interaction with a donor star in an X-ray binary system. The motion of the donor star around the black hole would produce a radial velocity sinusoidal curve which could be detected from the Doppler shifts of the photospheric absorption lines of the donor star. The semi-amplitude ( $K$ ) of the curve together with the binary period ( $P$ ) determine the mass function of the black hole (a lower limit to its mass), using Kepler’s third law:  $f_x = PK^3/(2\pi G)$ . Indeed, X-ray binaries were found in the late 1960s and the first black-hole candidate, Cyg X-1, in 1971 (Oda et al. 1971). Efforts in measuring the mass of Cyg X-1 were affected by uncertainties in the evolution of the massive donor star, and with a low mass function ( $f_x = 0.22 \pm 0.01 M_\odot$ ; Bolton 1975) this was not regarded as unequivocal evidence for a black hole (see Herrero et al. 1995 for the most recent work).

## 2. HUNTING FOR BLACK HOLES IN X-RAY NOVAE

In the 1980s the observational effort was turned to X-ray novae (XRNs, a sub-group of low-mass X-ray binaries). Unlike classical novae, XRNs are accretion-driven events that show disk outbursts with a typical rise of 8–10 mag in a few days and a subsequent decline over several months. After the XRN has subsided into quiescence, the accretion disk does not dominate the observed flux, rendering the companion star visible. The low-mass companion star allows the mass function of the black hole, a good approximation of the mass in a high-inclination system, to be determined. In the 1990s, X-ray satellites found 6 XRNs with identified companion stars in the optical (Nova Muscae 1991, Cheng et al. 1992; Nova Persei 1992, Casares et al. 1995a and references therein; Nova Sco 1994, Bailyn et al. 1995; Nova Vel 1993, Filippenko et al. 1999; GRO J1719-24, e.g., Ballet et al. 1993; XTE J1550-564, e.g., Smith et al. 1998).

The prototype target in the 1980s was A0620–00, but unfortunately its mass function was close to the maximum mass of a neutron star ( $f_x = 3.2 \pm 0.2 M_\odot$ ; McClintock and Remillard 1986). It was not until 1992 that a mass function of a candidate black hole in the XRN 1989, GS 2023+338, was found to be much heavier than the maximum mass of a neutron star ( $f_x = 6.08 \pm 0.06 M_\odot$ ; Casares et al. 1992). Since then, efforts have been directed toward measuring actual masses, thus producing the first observed mass distribution of black holes (Bailyn et al. 1998; Miller et al. 1998; for the theoretical distribution see Fryer 1999). The determination of the masses of stellar remnants after supernova explosions is essential for an understanding of the late stages of evolution of massive stars. Very recently, the first observational evidence for the progenitor, a supernova or hypernova with a mass  $> 30M_\odot$ , that produced the black hole of  $7.0 \pm 0.2 M_\odot$  in GRO J1655-40 was found with the Keck-I telescope (from high metal abundances that were presumably deposited onto the surface of the companion F5IV-star by the supernova explosion; Israelian et al. 1999).

---

Further author information: (Send correspondence to E. T. Harlaftis)

E. T. Harlaftis: E-mail: ehh@astro.noa.gr

A. V. Filippenko: E-mail: alex@astro.berkeley.edu

GRO J0422+32

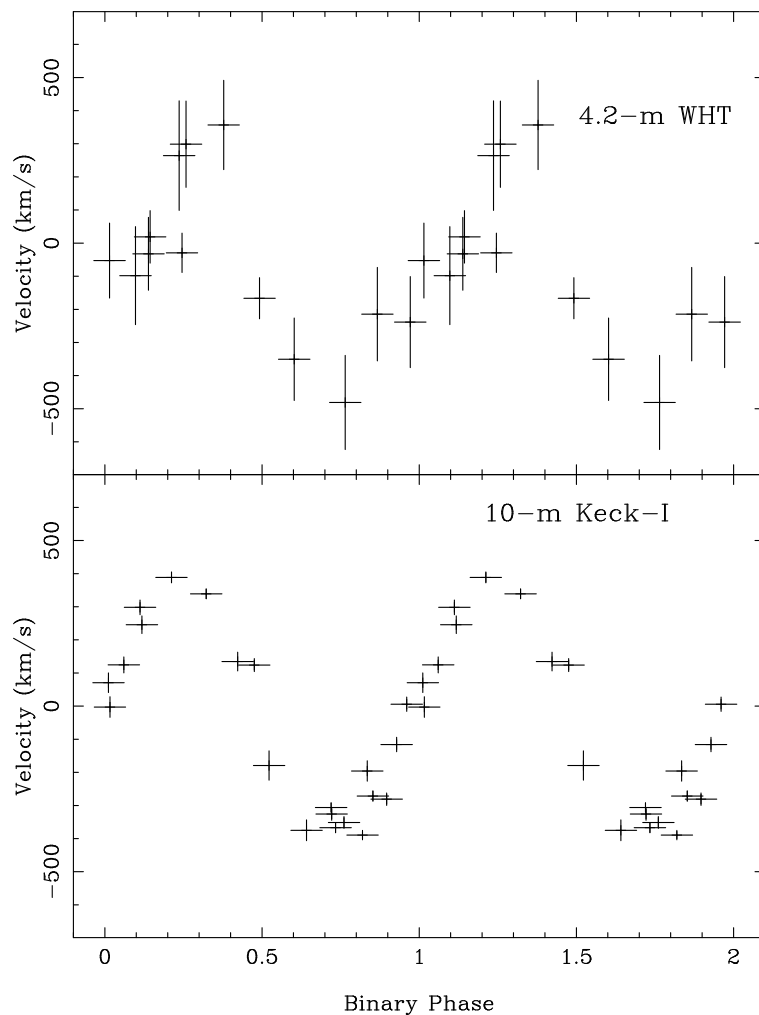


**Figure 1.** *Bottom:* the radial velocity curve of the companion star to the black hole GRO J0422+32 as extracted from spectra near H $\alpha$  with Keck-I/LRIS (Harlaftis et al. 1999). *Top:* the radial velocity curve of the companion star to the black hole GRO J0422+32 as extracted from 4.2-m WHT/ISIS near-infrared spectra (8450-8750 Å) (Casares et al. 1995a). The reduction in the individual measurement uncertainties is a factor of four using Keck-I. The sinusoidal fit to the radial velocities gives  $K = 338 \pm 39 \text{ km s}^{-1}$  with the WHT data and  $K = 372 \pm 10 \text{ km s}^{-1}$  with the Keck data for the radial velocity semi-amplitude of the companion star. This yields better accuracy in the estimate of the lower limit of the black hole's mass, from  $PK^3/(2\pi G) = 0.85 \pm 0.30 M_{\odot}$  to  $1.13 \pm 0.09 M_{\odot}$  for the low-inclination system GRO J0422+32. WHT data courtesy of Jorge Casares.

### 3. RADIAL VELOCITY CURVES

Utilizing the Doppler effect produced by the shifting photospheric lines due to the orbital motion of the companion star around the black hole, but now with the 10-m Keck-I and Keck-II telescopes, Filippenko and his collaborators have produced the four most accurate mass functions ( $f_x = 5.0 \pm 0.1 M_\odot$ ,  $1.2 \pm 0.1 M_\odot$ ,  $4.7 \pm 0.2 M_\odot$ ,  $3.2 \pm 0.1 M_\odot$ , respectively for GS 2000+25, GRO J0422+32, Nova Oph 1977, Nova Vel 1993; Filippenko et al. 1995a, 1995b, 1997, 1999). Figures 1 and 2 show the great improvement that the large aperture of Keck offers in comparison to 4-m-class telescopes in extracting radial velocity curves of the motion of the donor star around the black hole by cross-correlating main-sequence template spectra with the observed spectra.

### 4. THE MAIN SEQUENCE COMPANION STAR

The line broadening function affecting the absorption lines of the object spectra consists of the convolution of the instrumental profile (full width at half-maximum =  $108 \text{ km s}^{-1}$ ) with the companion star's rotational broadening profile (of width  $v \sin i$ ), with further smearing due to changes in the orbital velocity of the companion star during a given exposure. The exposure time for each object spectrum ( $T_{\text{exp}} \approx 25\text{--}40 \text{ min}$ ) resulted in orbital smearing of the lines up to  $2\pi K_c T_{\text{exp}}/P$ , which can range up to  $242 \text{ km s}^{-1}$ ; hence, the template spectra were subsequently smeared by the amount corresponding to the orbital motion through convolution with a rectangular profile and the resulting template spectrum was further broadened from 2 to  $150 \text{ km s}^{-1}$  by convolution with the Gray (1976) rotational profile. We scaled the blurred template spectrum by a factor  $0 < f < 1$  to match the absorption-line strengths in the Doppler-corrected average spectrum. Finally, the simulated template spectrum (i.e., smeared and broadened) was subtracted from the Doppler-corrected average spectrum of Nova Oph 1977 and  $\chi^2$  was computed from a smoothed version of the residual spectrum. The minimum  $\chi^2$  gives the optimal  $v \sin i$ ,  $f$ , and spectral type of the companion star (for more details see Harlaftis et al. 1996, 1997, 1999).

Figure 3 summarizes the procedure we follow to deconvolve the main-sequence spectrum from the target spectrum. The spectrum of a M2 V template (BD +44°2051) is shown at the bottom, binned to  $124 \text{ km s}^{-1}$  pixels (=4 pixels and similar to the instrumental resolution). This template was then treated so that its line profiles simulate those of the GRO J0422+32 spectra. The smearing in radial velocity due to the orbital line broadening while exposing are applied to individual copies of the M2 template, and these were subsequently averaged using weights identical to those corresponding to the GRO J0422+32 spectra. Next, a rotational broadening profile corresponding to  $v \sin i = 50 \text{ km s}^{-1}$  was applied; the result is the second spectrum from the bottom in Figure 3. The spectrum above is the Doppler-corrected average of the GRO J0422+32 data in the rest frame of the M2 V template. Finally, the residual spectrum is shown at the top after 0.61 times the simulated M2 V template ( $f = 0.61 \pm 0.04$  for M2; Table 4) was subtracted from the Doppler-shifted average spectrum. The M-star absorption lines and TiO bands are evident in the Doppler-corrected average, and they are almost completely removed by subtraction of the template spectrum (e.g., the Na I D line). Emission from He I  $\lambda 5876$  becomes prominent after subtraction of the M2 V template and weak emission from He I  $\lambda 6678$  is also present. Note that there is no evidence for Li I  $\lambda 6708$  absorption, to an equivalent width upper limit of  $0.13 \text{ \AA}$  ( $1\sigma$ ) relative to the original continuum, except in GS 2000+25 (see Martín et al. 1994 for lithium in X-ray binaries).

### 5. THE MASS RATIO OF THE BLACK HOLE BINARIES

Determination of the mass ratio (from the rotational broadening of the photospheric lines in the companion star) and the inclination (inferred from the ellipsoidal modulations of the companion star), when combined with the mass function, can fully describe the system's parameters and the masses of the binary components. The mass ratio  $q = M_2/M_1$  is found by measuring the rotational broadening of the absorption lines of the companion,  $v \sin i$ , through the relation

$$\frac{v \sin i}{K_c} = 0.46 [(1 + q)^2 q]^{1/3},$$

which is valid since the binary period is so short that the companion star is tidally locked to the black hole. We determined mass ratios for the first time for binaries as faint as 21 mag using the  $\chi^2$  optimization technique described in the previous section to extract the rotational broadening of the absorption lines of the donor star (Harlaftis et al. 1996, 1997, 1999). The complete results of the analysis of the Keck data are given in Table 1.

GS 2000+25

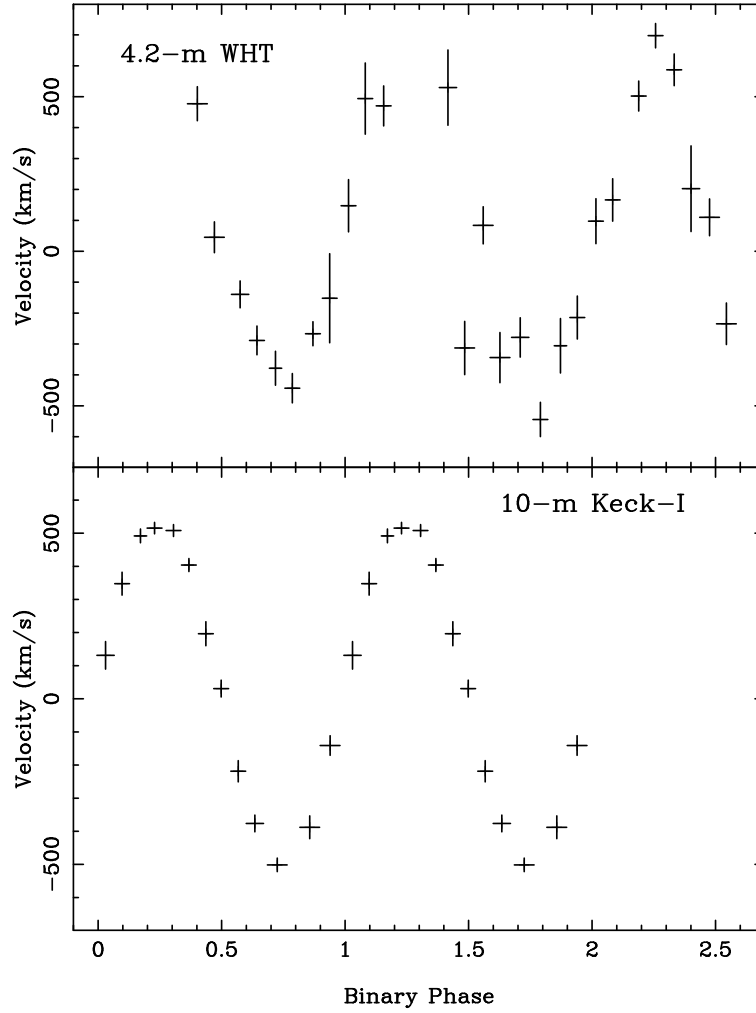


**Figure 2.** *Bottom:* the radial velocity curve of the companion star to the black hole GS 2000+25 as extracted from spectra near  $H\alpha$  with Keck-I/LRIS in just 1 night (Harlaftis et al. 1996). *Top:* the radial velocity curve of the companion star to the black hole GRO J0422+32 as extracted from 4.2-m WHT/ISIS in 3 nights (Casares et al. 1995b). The sinusoidal fit to the radial velocities gives  $K = 520 \pm 16 \text{ km s}^{-1}$  with the WHT data and  $K = 520 \pm 5 \text{ km s}^{-1}$  with the Keck data for the radial velocity semi-amplitude of the companion star. This yields better accuracy in the estimate of the lower limit of the black hole’s mass, from  $PK^3/(2\pi G) = 5.02 \pm 0.46 M_{\odot}$  to  $5.01 \pm 0.15 M_{\odot}$  for the high-inclination system GS 2000+25. WHT data courtesy of Jorge Casares.

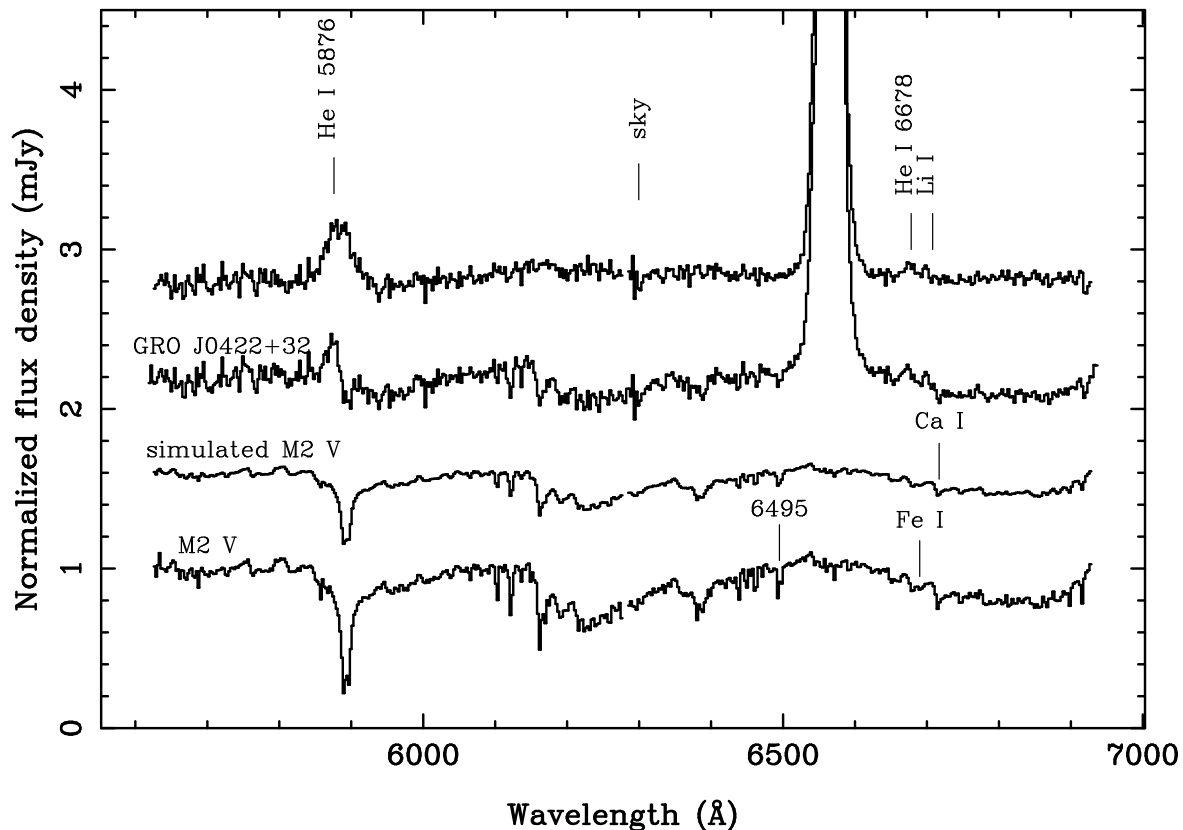


**Figure 3.**

Results of the technique followed to extract  $v \sin i$ ,  $f$ , and the spectral type of the companion star. From bottom to top: the M2 V template BD +44°2051, the M2 V template convolved with a complex profile to simulate effects of orbital smearing and rotational broadening ( $v \sin i = 50 \text{ km s}^{-1}$ ), the Doppler-shifted average spectrum of GRO J0422+32, and the residual spectrum of GRO J0422+32 after subtraction of the M2 V template times  $f = 0.61$ . The spectra are binned to  $124 \text{ km s}^{-1}$  pixels. An offset of 0.6 mJy was added to each successive spectrum for clarity. The residual spectrum is dominated by the disk spectrum (e.g., broad  $H\alpha$  and He I lines in emission). Several other lines are also marked, such as the characteristic Fe I+Ca I blend at 6495 Å in G–M stars, as well as the Ca I 6717 Å and Fe I lines surrounding the absent Li I line at 6707.8 Å.

**Table 1.** Keck-deduced parameters

	Oph 1977	GRO J0422+32	GS 2000+25	Vel 1993
$K_c$ (km s <sup>-1</sup> )	441±6	372±10	520±5	475±6
$f_x$	4.65±0.21	1.13±0.09	5.01±0.15	3.17±0.12
Spectral type	K5V±2	M2V <sup>+2</sup> <sub>-1</sub>	K5V <sup>+1</sup> <sub>-2</sub>	K8V±2
$f$ %	30±3	61±4	94±5	
$v \sin i$ (km s <sup>-1</sup> )	50 <sup>+17</sup> <sub>-23</sub>	90 <sup>+22</sup> <sub>-27</sub>	86±8	
$q$	0.014 <sup>+0.019</sup> <sub>-0.012</sub>	0.116 <sup>+0.079</sup> <sub>-0.071</sub>	0.042±0.012	

## 6. THE ACCRETION DISK

The accretion disk in its quiescent state has mainly been undetected so far by X-ray satellites but can be studied in the optical. Double-peaked Balmer profiles are observed with “S”-wave components either from the companion star (Nova Oph 1977) or the bright spot (GS 2000+25) and an H $\alpha$  emissivity law is observed, similar to that seen in dwarf novae. An imaging technique, Doppler tomography, shows the accretion disks in GS 2000+25, Nova Oph 1977 and GRO J0422+32 to be present (Fig. 4). Further, mass transfer from the donor star continues vigorously to the outer disk as evidenced by the “bright spot,” the impact of the gas stream onto the outer accretion disk in GS 2000+25 (Fig. 4; Harlaftis et al. 1996).

## REFERENCES

- Bailyn, C., et al. (1995) *Nature*, 378, 157
- Bailyn, C. D., Jain, R. K., Coppi, P., Orosz, J. A. (1998) *ApJ*, 499, 367
- Ballet, J., et al. (1993) IAUC No. 5874
- Bolton, C. T. (1975) *ApJ*, 200, 269
- Casares, J., et al. (1992) *Nature*, 355, 614
- Casares, J., et al. (1995a) *MNRAS*, 276, 35
- Casares, J., et al. (1995b) *MNRAS*, 277, L45
- Cheng, F. H., et al. (1992) 397, 664
- Filippenko, A. V., Matheson, T., Barth, A. J. (1995a) *ApJ*, 455, L139
- Filippenko, A. V., Matheson, T., Ho, L. C. (1995b) *ApJ*, 455, 614
- Filippenko, A. V., et al. (1997) *PASP*, 109, 461
- Filippenko, A. V., et al. (1999) *PASP*, 111, 969
- Fryer, C. L. (1999) *ApJ*, 522, 413
- Gray, D. F. (1976) *The Observations and Analysis of Stellar Photospheres* (New York: Wiley-Interscience), p. 373
- Harlaftis, E. T., Collier, S. J., Horne, K., Filippenko, A. V. (1999) *A&A*, 341, 491
- Harlaftis, E. T., Horne, K., Filippenko, A. V. (1996) *PASP*, 108, 762
- Harlaftis, E. T., Steeghs, D., Horne, K., Filippenko, A. V. (1997) *AJ*, 114, 1170
- Herrero, A., et al. (1995), *A&A*, 297, 556
- Israelian, G., et al. (1999) *Nature*, 401, 142
- McClintock, J. E., Remillard, R. A. (1986) *ApJ*, 308, 110
- Martín, E., et al. (1994) *ApJ*, 435, 791
- Miller, J. C., Shahbaz, T., Nolan, L. A. (1998) *MNRAS*, 294, L25
- Oda, M., et al. (1971) *ApJ*, 166, L10
- Smith, D. A., Marshall, F. E., Smith, E. A. (1998) IAUC No. 7008
- Zel’dovich, Ya. B., Novikov, I. D. (1966) *Sov. Physics – Uspekhi*, 8, 522

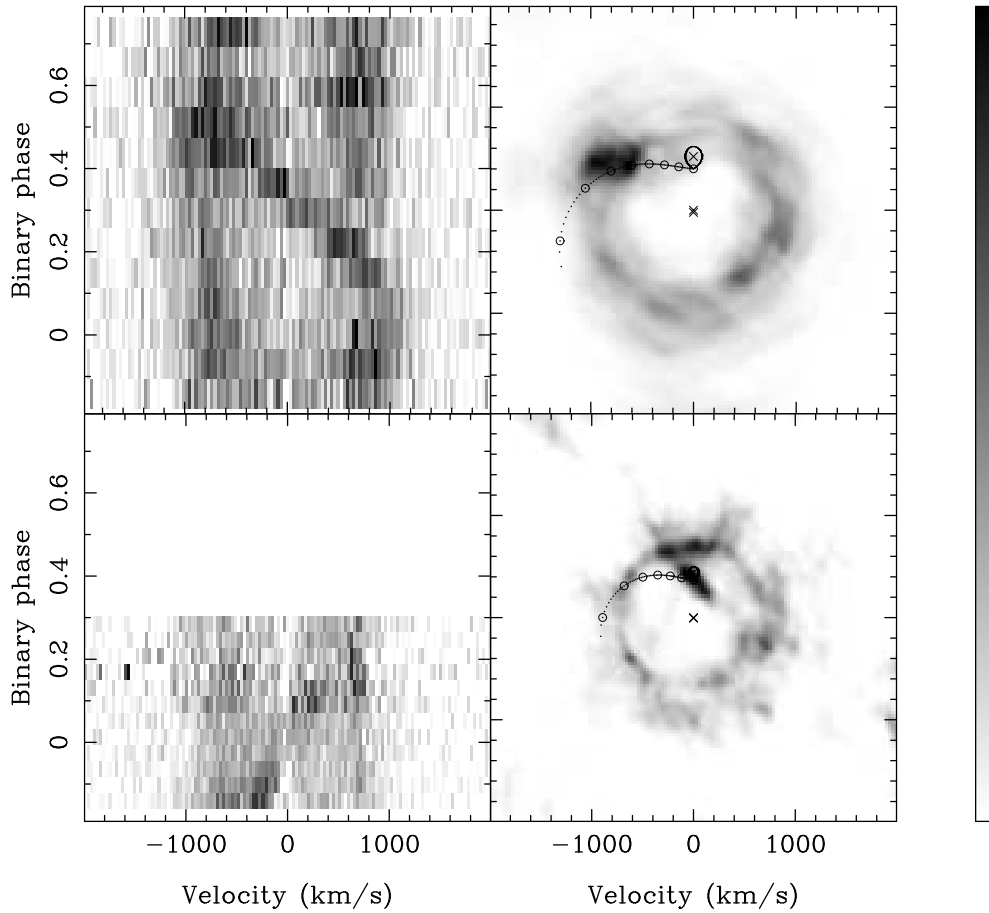


**Figure 4.** The  $H\alpha$  Doppler image (*top-right panel*) of the accretion disk surrounding the black hole GS 2000+25 (*bottom-right panel* for Nova Oph 1977), as reconstructed from 13 Keck-I/LRIS spectra which are also presented (*top-left panel; bottom-left panel* for the 12 spectra of Nova Oph 1977). By projecting the image in a particular direction, one obtains the  $H\alpha$  emission-line profile as a function of velocity; for example, projecting toward the top results in the profile at orbital phase 0.0, which has a blueshifted peak. The path in velocity coordinates of gas streaming from the dwarf K5 secondary star is illustrated. The GS 2000+25 Doppler map shows a bright spot, at the upper left quadrant, which results from collision of the gas stream with the accretion disk around the black hole. The Nova Oph 1977 map also shows a trace of an “S”-wave component which, however, is not resolved with clarity. The image was reconstructed by applying Doppler tomography, a maximum entropy technique, to the phase-resolved spectra, as described by Harlaftis et al. (1996, 1997, 1999).